Mathematical Modelling of Engineering Problems
Vol. 12, No. 7, July, 2025, pp. 2283-2297
Journal homepage: http://iieta.org/journals/mmep

Toward Smart and Flexible Spectrum Usage: Application of Horizontal Model Algorithm in Cognitive Radio Systems

Haider Farhi*, Abderraouf Messai

Laboratoire Satellite, Intelligence Artificielle, Cryptographie et Internet des Objets (SIACIO), Department of Electronics, University of Constantine 1 - Frères Mentouri, Constantine 25000, Algeria

Corresponding Author Email: haydar.ferhi@doc.umc.edu.dz

https://doi.org/10.18280/mmep.120709

Received: 29 April 2025
Revised: 14 June 2025
Accepted: 19 June 2025
Available online: 31 July 2025

Keywords:
Cognitive Radio, horizontal spectrum sharing, opportunistic access, Rayleigh fading, spectrum pooling, spectral efficiency, Time-Division Duplex, water-filling, wideband communication

ABSTRACT

The growing need for wireless communication services has resulted in a pressing need for more enhanced exploitation of available spectrum bandwidth. Cognitive Radio (CR) technology emerges as a potential solution, facilitating secondary users, in their ability to opportunistically access underutilized spectral resources without causing harmful interference to primary users. In this paper, we propose and analyze a horizontal spectrum-sharing model for CR systems operating in wideband environments. Unlike traditional orthogonal access schemes, the horizontal model enforces exclusive sub-band transmission per user in the Time-Division Duplex (TDD) framework, combined with the water-filling power allocation strategy to maximize spectral efficiency. We develop an analytical framework to characterize the spectral efficiency and capacity achievable by the proposed model and assess its asymptotic behavior under Rayleigh fading channels. Extensive simulations are conducted to validate the theoretical findings, comparing the horizontal model to the classical orthogonal model across various Signal-to-Noise Ratio (SNR) regimes. Results demonstrate that the horizontal sharing approach significantly improves spectral efficiency, especially in low-SNR conditions, and converges to the orthogonal performance in high-SNR environments. This work provides valuable insights into the design of future CR systems, highlighting the advantages of opportunistic spectrum pooling strategies for enhancing overall network performance.

1. INTRODUCTION

The exponential rise in wireless communication technologies has significantly increased the demand for radio spectrum, a limited and tightly regulated resource [1-3]. Despite this growing demand, various studies and practical observations consistently indicate that substantial portions of the licensed spectrum are often left unused across different times, locations, and frequency bands. This persistent underutilization highlights a pressing challenge of enhancing spectrum efficiency while ensuring that the rights and operations of licensed (primary) users are preserved [4, 5].

Traditional spectrum management relies on static allocation policies, where frequency bands are exclusively assigned to specific services or operators [6]. While this model simplifies regulation, it leads to significant spectral wastage, particularly in frequency bands reserved for applications with variable or sporadic usage. In response to this inefficiency, the research community and regulatory bodies, such as Federal Communications Commission (FCC), have proposed more dynamic and intelligent methods for spectrum access [4].

One prominent solution is CR concept, which enables secondary (unlicensed) users to opportunistically access unused spectrum portions while ensuring no detrimental interference to primary users. CRs rely on spectrum sensing, adaptive transmission, and learning mechanisms to identify and exploit spectrum holes in real time. The potential of CR systems has led to the development of various frameworks, including Dynamic Spectrum Access (DSA), Opportunistic Spectrum Access (OSA), and cooperative sensing techniques [7].

In this context, this work selects several recent and noteworthy studies for analysis, aiming to identify research gaps in this area. For instance, Bouhafs et al. [6] proposed a spectrum management platform for 6G networks based on a sharing economy model. Using a simulated dense Internet of Things (IoT) deployment with 5G base stations and Wi-Fi 802.11ah access points, they demonstrated dynamic spectrum trading through Software Defined Wireless Networking (SDWN), heterogeneous spectrum programming, and a brokering interface. The approach improves spectral efficiency, Signal to Interference plus Noise Ratio (SINR), and reduces connectivity denial compared to traditional static 5G allocation. However, its limitations include reliance on simple trading algorithms and lack of real-time, interference-aware control.

Table 1. Summary of related works on spectrum management approaches

Ref.	Year	Materials (System/Setup)	Methods	Advantages	Limitations (vs. Horizontal Sharing in Cognitive Radio Networks (CRNs))
[6]	2022	Simulated dense IoT with 5G BSs and Wi-Fi 802.11ah APs	SDWN, spectrum brokering, heterogeneous programming	↑ Spectral efficiency, ↑ SINR, ↓ denial rate	No exclusive sub-band use, lacks interference-aware control and water-filling
[8]	2022	Simulated 10-device SAGIN setup with varying priorities and bandwidths	HNOGA: GA + MGA + niche + orthogonal crossover	Fast convergence, strong stability, superior optimization	No real-time power control or exclusive allocation; not adaptive to dynamic CRN needs
[9]	2023	Centralized MATLAB model with fuzzy logic and smart sensing	SSDSM with periodic sensing + decision support	↑ Throughput, ↓ delay, ↑ QoS	Assumes ideal sensing; lacks decentralization and dynamic multi-user adaptability
[10]	2024	2-IoT device distributed CSS with no fusion center	Energy detection, PBPO, dynamic programming	↑ Sensing accuracy, ↓ sensing cost, scalable	Fixed cooperation structure; limited adaptability to heterogeneous/dynamic spectrum conditions
[11]	2024	IoV system with cognitive vehicles, PBS, and fusion center	Double-threshold energy detection; OR/AND fusion rules based on traffic	↑ Detection accuracy under low SNR, ↓ false alarms, energy efficient	Centralized fusion, static grouping/rules; lacks flexibility for complex, time-varying vehicular scenarios

Unlike horizontal spectrum-sharing models in CRNs, this approach lacks exclusive sub-band access and intelligent power allocation, underscoring the added value of horizontal models in managing interference and optimizing performance.

Meng et al. [8] proposed a Hybrid Niche Orthogonal Genetic Algorithm (HNOGA) to allocate spectrum for diverse devices with varying frequency needs in integrated space–air–ground networks. They used a simulated system consisting of ten frequency-using devices with varying bandwidths, transmission powers, and service priorities. The approach is based on mathematical modeling and optimization, integrating a standard genetic algorithm with a micro genetic algorithm for enhanced local search capabilities.

It also adopts niche techniques for population diversity, and an orthogonal uniform crossover operator for efficient solution generation. The main advantages of this approach include faster convergence, higher stability, and superior optimization performance compared to traditional genetic, ant colony, and greedy algorithms. However, the method lacks key characteristics found in horizontal spectrum-sharing models for CRNs, specifically, it does not enforce exclusive sub-band allocation or real-time power control strategies like water-filling. Consequently, while effective within its scope, the method may be less adaptable to dynamic or interference-sensitive environments where Cognitive Radio (CR) thrives, highlighting the added value and relevance of our proposed horizontal sharing framework.

Fraz et al. [9] proposed a Smart Sensing Enabled Dynamic Spectrum Management (SSDSM) framework for CRNs using a centralized model simulated in MATLAB. The system employs fuzzy logic decision support and periodic smart sensing to optimize spectrum allocation, reduce energy consumption, and improve QoS. Advantages include increased throughput, reduced service delay, and fewer handoffs compared to baseline methods. However, the approach assumes ideal sensing and centralized coordination, limiting its effectiveness in decentralized, dynamic multi-user scenarios, highlighting the need for more adaptable and interference-aware spectrum sharing strategies.

Wu et al. [10] developed a distributed cognitive IoT model for Cooperative Spectrum Sensing (CSS), involving two IoT devices that use energy detection and sequential decision-making without a centralized fusion center. They applied dynamic programming and a Person-By-Person Optimization (PBPO) method to minimize the combined cost of sensing time and decision errors, formulating and solving a joint optimization problem. This approach improves sensing accuracy and reduces average cost, making it suitable for scalable, heterogeneous IoT environments. However, the method is constrained by its reliance on fixed cooperation structures and lacks adaptability to diverse, dynamic spectrum usage patterns, emphasizing the importance of developing more adaptive and environment-sensitive spectrum access mechanisms.

Du and Wang [11] introduced a double-threshold cooperative spectrum sensing algorithm tailored for CR applications within the Internet of Vehicles (IoV), utilizing a system model that includes cognitive vehicles, a Primary Base Station (PBS), and a fusion center. The method enhances traditional energy detection by introducing dual thresholds, which are dynamically adjusted based on noise uncertainty, and applies collaborative decision-making using OR and AND fusion rules depending on traffic conditions. This approach significantly improves detection accuracy, especially under low SNR and high-noise environments, and reduces false alarms compared to single-threshold methods. Advantages of the proposed method include adaptability to fluctuating vehicular and environmental conditions, reduced energy consumption, and higher reliability in detecting spectrum availability. However, the method still faces limitations due to its dependence on centralized fusion decisions, fixed vehicle groupings, and static rule-based adaptation, which restrict its flexibility and responsiveness in more complex and heterogeneous communication landscapes, underscoring the importance of exploring mechanisms that can better accommodate dynamic interactions and varying operational contexts. To identify research gaps and highlight the unique value of our horizontal spectrum-sharing model, Table 1 summarizes key recent studies.

Despite notable advancements in CR research, several critical limitations persist in current spectrum management approaches. As summarized in Table 1, many recent methods still exhibit structural or operational drawbacks that limit their applicability in real-world, dynamic environments. For instance, the SSDSM framework presented by Fraz et al. [9] employs fuzzy logic and periodic sensing in a centralized MATLAB setup, achieving gains in throughput and QoS. However, it assumes ideal sensing conditions and centralized

coordination, which can hinder adaptability and scalability in decentralized, heterogeneous networks. Similarly, the distributed cooperative spectrum sensing model in reference [10] introduces energy detection and dynamic programming to improve sensing accuracy and reduce cost, but its reliance on fixed cooperation structures limits flexibility in diverse or evolving spectrum conditions. The double-threshold cooperative algorithm proposed by Du and Wang [11] improves detection accuracy under low SNR and reduces false alarms in vehicular networks, yet it still depends on centralized fusion decisions and static rule configurations, restricting responsiveness in time-varying environments. Furthermore, methods such as those studies [6, 8] focus on optimization and spectrum brokering, but fall short in interference-aware power control and exclusive sub-band access. Overall, these limitations highlight the necessity for more robust, decentralized, and horizontally coordinated CRN strategies that support intelligent sub-band allocation, dynamic cooperation, and adaptive interference mitigation to maximize system-wide spectral efficiency. In summary, while prior studies have explored dynamic access and optimization strategies, they often lack exclusive sub-band allocation, real-time power control, or decentralized operation. This paper proposes a novel horizontal spectrum-sharing model that combines exclusive sub-band usage with water-filling power allocation in a TDD CR system. Analytically evaluated under Rayleigh fading and validated via simulations, the model enhances spectral efficiency, especially at low SNR, while supporting scalable, decentralized access in wideband environments.

To address these shortcomings, this paper proposes a horizontal spectrum-sharing model that redefines access dynamics in CR systems. Unlike previous models, our approach enforces exclusive sub-band access per user within TDD framework (see Figure 1). Figure 1 illustrates the horizontal spectrum-sharing concept, where each user is assigned a distinct sub-band within the TDD frame, preventing simultaneous transmissions on the same sub-band and minimizing interference. This exclusivity, paired with a water-filling power allocation strategy, enables precise interference control and maximizes collective system efficiency. The model prioritizes coordinated multi-user access, ensuring that at most one user transmits on any given sub-band at a time, which sharply contrasts with shared-access strategies employed in earlier studies.

We explore the application of this model in a heterogeneous wideband CR environment, where both primary and secondary users seek communication opportunities across various receivers. Assuming perfect spectrum sensing, the system dynamically assigns sub-bands based on real-time availability and user demand. By enforcing one-user-per-sub-band transmission, our framework significantly enhances spectral efficiency and total system capacity, providing a robust alternative to traditional access schemes. Through simulation and analysis, we demonstrate that horizontal sharing mitigates interference more effectively and also achieves superior performance in terms of global spectral utilization when compared to conventional spectrum access methods. Compared to previous methods [6, 8, 9], which often lack exclusive sub-band access or rely on centralized spectrum decisions, our approach enables fully decentralized allocation with exclusive access per sub-band and dynamic power control. This combination allows for efficient operation in fluctuating environments, particularly under noise-limited (low-SNR) conditions.

This paper is organized as follows: Section 2 presents Materials and Methods, starting with an analysis of spectral efficiency in CR environments, followed by a description of the channel model. We then introduce the CR protocol that supports horizontal sub-band assignment, and formulate the detection problem along with its integration into the network operation. Next, we perform a detailed spectral efficiency analysis and assess the asymptotic performance of the proposed method. Section 3 discusses the simulation results and comparative performance evaluation. Section 4 provides the conclusions of this work and potential opportunities.

Throughout this paper, we refer to our proposed approach as the *horizontal spectrum-sharing model*, which enables decentralized and interference-aware access through exclusive sub-band allocation in a TDD framework. The term *spectrum pooling* is used more generally to describe the dynamic reuse of sub-bands across users, a behavior inherently supported by the horizontal model. We use *cognitive users* to denote secondary users in a CRN who opportunistically access spectrum while avoiding interference with licensed (primary) users.

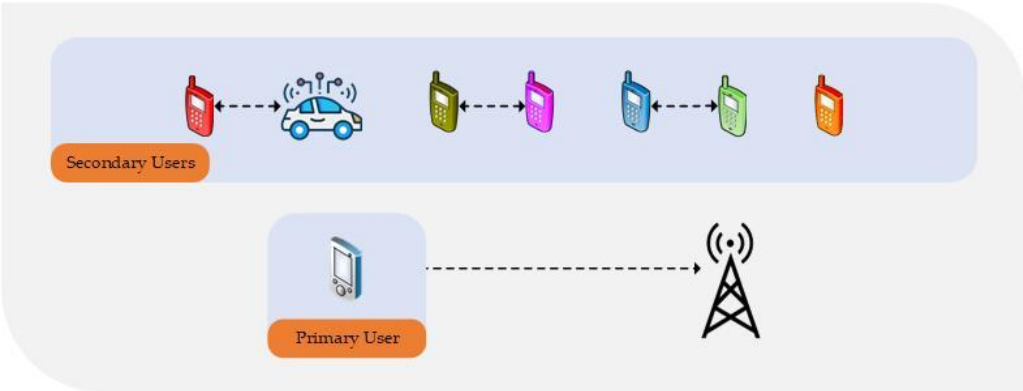

Figure 1. Wheel slip behavior under the proposed control algorithm

2. MATERIALS

Building upon the limitations identified in previous CR models and the motivations outlined in the introduction, this section presents the core framework and technical components of the proposed horizontal spectrum-sharing model. We begin by analyzing the spectral efficiency challenges inherent to wideband CR systems operating under Rayleigh fading

conditions. Then, we detail the adopted channel model, highlighting the assumptions made regarding channel state information and signal propagation. Following this, we introduce the CR protocol specifically designed for coordinated sub-band assignment, which enforces a one-user-per-sub-band transmission policy to maximize spectral efficiency. We also describe the detection mechanism that enables users to dynamically sense and adapt to the spectrum environment. After establishing these foundational elements, we develop an analytical framework to evaluate both the spectral efficiency and system capacity under finite and asymptotic conditions. Through this structured methodology, we aim to rigorously assess the performance benefits of horizontal spectrum pooling in CNRs.

2.1 Spectral efficiency

In spectrum pooling systems, channel allocation strategies are designed to give priority to primary users. Secondary users are then allocated to the identified spectrum gaps. These holes are assumed to be empty within the sub-band range. Therefore, secondary users fill these gaps as long as they reach the desirable transmission power level. More specifically, the spectrum is divided into N sub-bands and each user l tries to transmit using an optimal power control strategy. The operation of the system is considered within a wideband context. Consequently, the N sub-bands of CR channel extend to infinity ($N \to \infty$). The channel is assumed to have components that experience fading and vary slowly over time, where the receiver is capable of sensing and tracking the channel fluctuations. The channel fluctuations, represented by the channel gain h for each user l and are assumed constant over a block duration so that they can be retained while the block is processed.

Under these assumptions, the average capacity of user l in bits/s/Hz is given by Eq. (1) [12], where $p_l(t)$ denotes the power allocated by user l as a function of the fading coefficient t, and N_0 represents the noise power spectral density.

$$C_{l,\infty} = \int_0^\infty \log_2\left(1 + \frac{p_l(t)\cdot t}{N_0}\right) e^{-t}\, dt \tag{1}$$

To maximize the transmission rate when optimal power control is applied, the power $p_l(t)$ is subjected to the average power constraint as in Eq. (2), where γ_0 is the water-filling power allocation threshold (also called the cut-off parameter). Thus, the spectral efficiency of CR in Rayleigh fading channels can be properly modeled under these conditions.

$$\int_0^\infty \left(\frac{1}{\gamma_0} - \frac{N_0}{t}\right) e^{-t}\, dt = 1 \tag{2}$$

2.2 Channel model

The discrete baseband frequency model at the receiver RI (see Figure 1) is given by Eq. (3), where h_i^l is the block fading process of user l on sub-band i, s_i^l represents the signal transmitted by user l on sub-band i, $p_i^l(h_i^l)$ refers to the power control function of user l on sub-band i, and n_i^l is the additive white Gaussian noise on the i-th sub-band.

$$y_{RI}^i = h_i^l \sqrt{p_i^l(h_i^l)} s_i^l + n_i^l, \quad \text{for } i = 1, \dots, N \text{ and } l = 1, \dots, L \tag{3}$$

It is assumed that the channel remains constant over the coherence time, which corresponds to a single fading block (i.e., coherent communication). The assumption of coherent reception is reasonable when the fading is slow enough to allow the receiver to track the channel variations. Statistically, the channel gains h_l are modeled as independent and identically distributed (i.i.d.) Rayleigh fading random variables, both across users l and sub-bands i. The wideband CR channel in the horizontal sharing model, with multiple secondary users operating over N sub-bands in parallel, is represented schematically in Figure 1. In the special case of a single secondary user employing orthogonal access across the available sub-bands, the system can be modeled as shown in Figure 2. Figure 2 depicts the orthogonal access scenario as a baseline model, where a single secondary user accesses non-overlapping sub-bands, eliminating interference but limiting spectral efficiency. This representation simplifies the analysis while capturing the essential aspects of dynamic sub-band selection in CR environments.

The Rayleigh fading assumption implies the following normalization presented by Eq. (4).

$$\mathbb{E}[|h_l|^2] = 1, \quad \text{for } l = 1, \dots, L \tag{4}$$

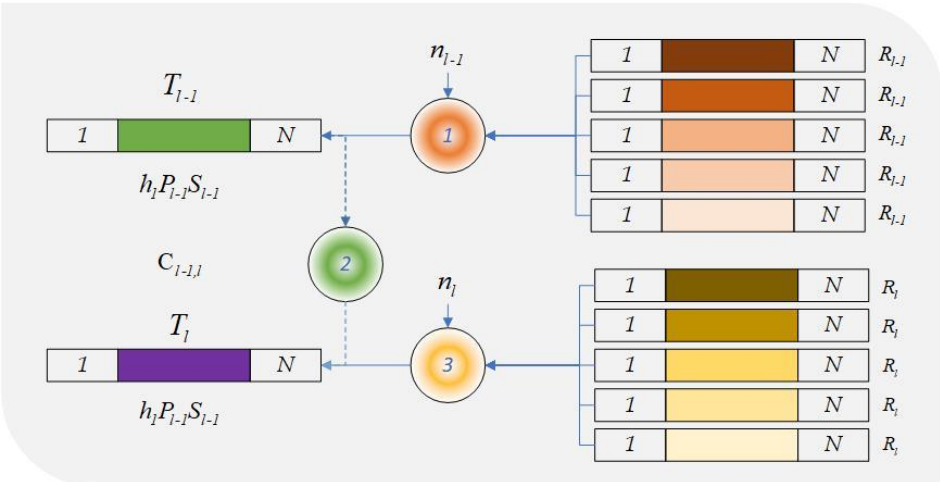

Figure 2. CR channel model in a wideband/multi-band context with primary and secondary users operating under horizontal spectrum sharing

2.3 CR protocol

Several modern studies have investigated the spectral efficiency of cognitive systems relative to traditional settings, allowing cognitive users to transmit simultaneously with primary users over the same frequency band.

Various studies in CR field networks have explored different strategies to enhance spectral efficiency and enable coexistence between primary and secondary users [2, 13, 14]. In some approaches, cognitive users are assumed to have prior knowledge or partial awareness of the primary users' transmissions, allowing for more intelligent adaptation of their communication strategies. Other frameworks consider cooperative strategies, where both primary and secondary systems collaboratively design their encoder-decoder structures to mitigate mutual interference and optimize performance. However, in practical deployments, primary systems are typically unaware of the existence of cognitive users and operate independently according to the requirements of primary network users. Consequently, CRs must autonomously sense their communication environment and adapt their transmission parameters to maximize the quality of service for secondary users while minimizing interference to primary transmissions. Recent research proposes protocols where primary and secondary users share the spectrum asynchronously, often under the assumption that each user only has knowledge of its own channel state and can detect the occupancy of the spectrum through spectrum sensing mechanisms in multiband or wideband systems [2, 13, 14].

Under our proposed protocol, cognitive users listen to the wireless channel and determine in real-time which parts of the spectrum are occupied. They then continuously adapt their signal accordingly. After this detection phase, a comparison algorithm is introduced between users based on capacity. Ultimately, only one secondary user fills the detected spectral holes, maximizing capacity, as the system operates in TDD mode. In TDD, transmission and reception occur over the same frequency band but at different times. Each transmitter for user l, T_l, where, $l = 1, \dots, L$ estimates the pilot sequence from receiver R_l to determine the channel gain h_l. It is assumed that the channel remains constant between the time of estimation and transmission. Thus, each user l knows only their own channel gain h_l and the statistical properties (probability distribution) of other links. An especially interesting goal in this context, when employing a listen-before-talk strategy, is to reliably detect sub-bands currently available for a given user, saving them for upcoming transmissions. This knowledge can be acquired either centrally, via a database maintained by the regulator or another authority [15-17], or via an additional signaling channel for collision detection to prevent cognitive users from transmitting simultaneously.

Specifically, the primary user arrives first and estimates its channel gain. Then, the cognitive users synchronously compare their capacities to select the one with the maximum capacity, thus avoiding simultaneous transmissions and enhancing the system's overall capacity. Secondary users arrive randomly (for example, following a Poisson process) and estimate their channel links. In this new framework, the primary user remains ignorant of the cognitive users. Cognitive users, capable of accurately sensing the spectral environment over a wide bandwidth, initiate communication only when it does not interfere with primary users. Thus, under our opportunistic approach, a device transmits on a certain sub-band only if no other user is doing so. In an asynchronous context, the probability of two users transmitting simultaneously is negligible.

The sensitive algorithms for cognitive users and the performance analysis of such an approach are proposed [15]. In the rest of this paper, we adopt this framework to analyze the achievable performance of the system in terms of capacity, spectral efficiency gains, and the maximum number of possible communication pairs. Such a simple and precise modeling provides a clear understanding of the real benefits of spectrum pooling technology. Despite the excitement generated by CRs, many theoretical questions about their performance limits remain unanswered.

To evaluate the theoretical performance limits of such systems, three capacity metrics are commonly discussed in the literature. Comprehensive reviews of these measures can be found in several prior works. For the proposed protocol, the most relevant performance indicator is the instantaneous capacity per sub-band, expressed in bits/s/Hz, also known as spectral efficiency, as defined in Eq. (5). The sum here is taken over the stationary instantaneous distribution of the fading channel for each user l. The instantaneous capacity determines the maximum achievable rate across all fading states without delay constraints.

$$C_l = \frac{1}{N}\sum_{i=1}^{N} \log_2\left(1 + \frac{p_l^i \left|h_l^i\right|^2}{N_0}\right), \quad l = 1, \dots, L \tag{5}$$

In our work, we transmit using optimal power allocation under a total power budget constraint to maximize each user's transmission rate. When Channel State Information (CSI) is available at the transmitter, users adapt their transmission strategies accordingly. The corresponding optimal power allocation is the well-known water-filling strategy, expressed as in Eq. (6), where γ_0 is the Lagrange multiplier satisfying the average power constraint presented in Eq. (4). Without loss of generality, we assume $\overline{P} = 1$ in the remainder of this document.

$$p_l^i = \left(\frac{1}{\gamma_0} - \frac{N_0}{\left|h_l^i\right|^2}\right)^+ \tag{6}$$

$$\frac{1}{N}\sum_{i=1}^{N} p_l^i = \overline{P} \tag{7}$$

The water-filling strategy offers significant performance gains compared to constant-power strategies, particularly at low SNR. When transmission power is limited, it is more efficient to concentrate energy on the strongest sub-channel rather than spreading it across all modes. At high SNR, the transmitter tends to distribute power across all available sub-bands. This behavior has been similarly observed [16, 17]. It is important to note that even though a water-filling strategy is adopted in this analysis, it does not restrict the proposed protocol. As mentioned earlier, in spectrum pooling implementations, cognitive users operate on the remaining sub-bands left by the licensed system, resulting in a binary channel assignment, as depicted in Figure 2 and Figure 3. Figure 3 illustrates the binary sub-band allocation in a wideband CR system, where each available sub-band is either fully used or left idle based on channel conditions and spectrum availability.

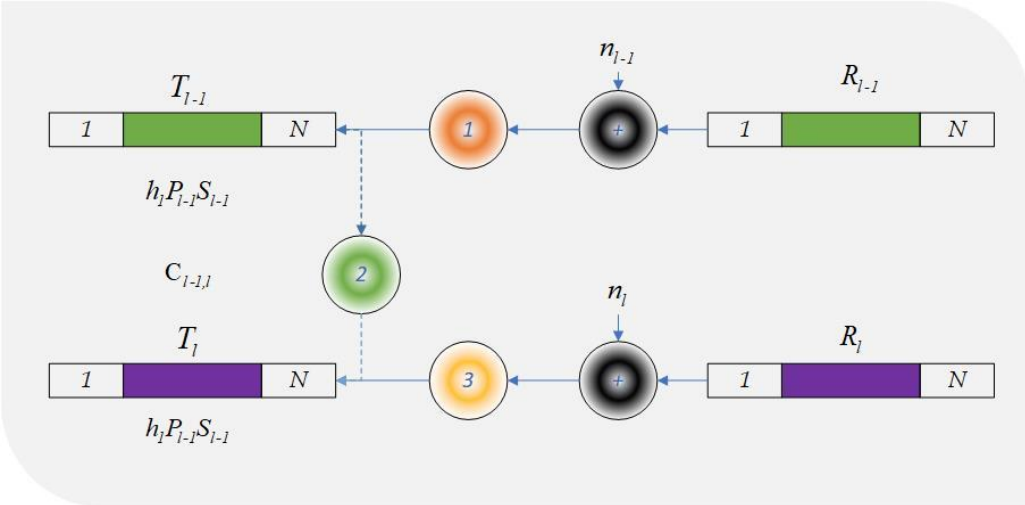

Figure 3. CR channel in a wideband/multi-band context with N sub-bands and a single secondary user (orthogonal access)

For clarity, consider an example where $N = 10$ sub-bands. The primary user always has priority access to the entire bandwidth, while cognitive users adapt their signals to fill detected gaps according to their priority order. Initially, the primary user maximizes its rate based on its channel process. As previously described in Eq. (1) five secondary users at any instant t with channel gains exceeding a threshold $\gamma_0 N_0$ wish to transmit on sub-band Ψ_2. However, the TDD principle ensures that only one user transmits at a time. Our approach respects this principle by comparing the capacities of all cognitive users wishing to communicate. The secondary user with the maximum capacity $C_{\max}$ senses the spectrum and transmits only on inactive sub-bands. Subsequently, the next cognitive user senses the residual sub-bands left unused by prior transmissions, adapting their signal to fill these gaps (Ψ_3, Ψ_4, etc.) until full spectrum utilization is achieved.

2.4 Detection problem

Until now, the focus has been on pairwise communications between transmitters and receivers. We now examine inter-transmitter communications to analyze the detection problem. For this purpose, we assume that the baseband model is discrete in time over a period T, where each user l for $l = 2, \dots, L$ operates over N sub-bands as described in Figure 2. The received signal at user l can be expressed as in Eq. (8), where $c_{l-1,l}^{i}(k)$ represents the block fading process from user $l-1$ to user l on the i-th sub-band at time k. The term $p_{l-1}^{i}(h_{l-1}^{i})$ denotes the power control function of user $l-1$ on sub-band i, $s_{l-1}^{i}(k)$ is the transmitted signal from user $l-1$ on sub-band i, and $n_{l-1}^{i}(k)$ represents the additive white Gaussian noise on the i-th sub-band at time k. While perfect spectrum sensing is assumed in this model to facilitate tractable analysis, we acknowledge that this is an idealized condition. In practice, sensing may be subject to noise uncertainty, misdetection, or false alarms. As such, our results represent a theoretical upper bound on system performance. Future work will extend this framework to account for realistic sensing imperfections and explore robust detection strategies.

$$\mathbf{y}_l^i(k) = c_{l-1,l}^{i}(k)\sqrt{p_{l-1}^{i}(h_{l-1}^{i})}s_{l-1}^{i}(k) + n_{l-1}^{i}(k), \qquad (8)$$

We further assume that $0 \le k \ll \beta T$, meaning that the coherence time is sufficiently large for the channel to remain constant over the samples and only change to a new independent value after some duration (block fading model). The sensing techniques proposed rely on the assumption that all devices operate under a unified standard and know the pilot sequences used by the other users. As mentioned earlier, in this work, the spectrum pooling behavior is assumed to allow only one user to transmit simultaneously over the same sub-band. to support TDD operation, synchronization is achieved through pilot-based channel estimation and a distributed scheduling protocol, where each user independently estimates its channel and compares local capacities before transmission. Time slots are aligned using a shared reference signal or frame structure, ensuring that sub-band assignments remain collision-free.

Thus, the received signal at user l can also be rewritten conditionally as in Eq. (9). Assuming that βT is an integer equal to M and that βT is sufficiently large, the average received power during the detection period at receiver R_l is presented by Eq. (10), where the first case represents the sum of signal and noise when transmission occurs, and the second case represents pure noise otherwise.

$$\mathbf{y}_l^i(k) = \begin{cases} c_{l-1,l}^{i}(k)\sqrt{p_{l-1}^{i}(h_{l-1}^{i})}s_{l-1}^{i}(k) + n_{l-1}^{i}(k), & \text{if} \quad p_{l-1}^{i} \neq 0 \\ n_{l-1}^{i}(k), & \text{otherwise} \end{cases} \qquad (9)$$

$$\lim_{M\to\infty} \frac{1}{M}\sum_{k=1}^{M}\left|\mathbf{y}_l^i(k)\right|^2 = \begin{cases} \left|c_{l-1,l}^{i}\right|^2 P_{l-1}^{i} + N_0, & \text{if} \quad p_{l-1}^{i} \neq 0 \\ N_0, & \text{otherwise} \end{cases} \qquad (10)$$

Consequently, to determine which part of the spectrum is used, a cognitive user detects the received power and compares it with the known noise power N_0. The main difficulty in this detection process is to obtain an accurate estimation of the noise variance. In the context of spectrum pooling mechanisms, it is necessary to employ a channel detection method that continuously senses the channel. Furthermore, channel detection must be performed with a very high probability of correct detection to ensure a very low probability of interference with the primary system, as highlighted in recent works [18, 19].

2.5 Spectral efficiency analysis

We first attempt to identify the set of sub-bands detected as occupied by user l as in Eq. (11), where Ψ_l satisfies the following properties in Eq. (12). Then, the capacity per band for user l with N sub-bands is given by Eq. (13).

$$\Psi_l = \left\{ i \in \{1, \dots, N\} \,|\, p_{l-1}^i \neq 0 \right\} \tag{11}$$

$$\begin{cases} \Psi_1 = \emptyset, \\ \bigcup_{l=1}^{L+1} \Psi_l \subseteq \{1, \dots, N\}, \\ \bigcup_{l=1}^{L+1} \Psi_l = \emptyset \end{cases} \tag{12}$$

$$C_{l,N} = \frac{1}{\text{card}(\Omega_l)} \sum_{i \in \Omega_l} \log_2 \left(1 + \frac{p_l^i \left| h_l^i \right|^2}{N_0} \right) \tag{13}$$

Here, Ω_l represents the set of remaining inactive sub-bands detected by user l, namely, as presented in Eq. (14).

$$\Omega_l = \left\{ i \in \{1, \dots, N\} \right\} \cap \overline{\bigcup_{k=1}^{l-1} \Psi_k} \tag{14}$$

For a given number of sub-bands N, the optimal power allocation that maximizes the transmission rate for user l solves the following optimization problem depicted in Eq. (15), subject to the average power constraint in Eq. (16).

$$\max_{p_l^1, \dots, p_l^I} C_{l,N} \quad \text{for} \quad l \in [1, L] \tag{15}$$

$$\begin{cases} \dfrac{1}{\text{card}(\Omega_l)} \displaystyle\sum_{i \in \Omega_l} p_l^i = 1 \\ p_l^i \geq 0 \end{cases} \tag{16}$$

The optimal power control policy is derived in Eq. (5). It is noteworthy that the maximum number of users L authorized in such a system must satisfy the condition that $\text{card}(\Omega_L) \neq 0$. We now study the derivation of the achievable spectral efficiency for this system. The spectral efficiency per band for user l is given by Eq. (17). By multiplying and dividing Eq. (17) by card (Ω_l), we obtain the formula in Eq. (18).

$$\Phi_{l,N} = \frac{1}{N} \sum_{i \in \Omega_l} \log_2 \left(1 + \frac{p_l^i \left| h_l^i \right|^2}{N_0} \right) \tag{17}$$

$$\Phi_{l,N} = \begin{cases} C_{1,N} \quad \text{if} \quad l = 1 \\ \dfrac{\text{card}(\Omega_l)}{N} \cdot C_{l-1,N} \quad \text{for} \quad l \in [2, L] \end{cases} \tag{18}$$

Since the primary user benefits from the entire bandwidth, we have $\text{card}(\Omega_1) = N$. As expected, when $l = 1$, the spectral efficiency without cognition equals the primary user's capacity $C_{1,N}$. We define $\Delta_{l,N}$ as the bandwidth gain factor for user l over N sub-bands, as presented by Eq. (19). In other words, the bandwidth gain factor represents the fraction of the unoccupied band allocated to user l. Thus, the spectral efficiency per band for user l can be expressed as in Eq. (20).

$$\Delta_{l,N} = \frac{\text{card}(\Omega_l)}{N}, \quad \text{for} \quad l \in [1, L] \tag{19}$$

$$\Phi_{l,N} = \begin{cases} \Delta_{1,N} C_{1,N}, \quad \text{if} \quad l = 1 \\ \Delta_{l,N} C_{l-1,N}, \quad \text{for} \quad l \in [2, L] \end{cases} \tag{20}$$

Finally, the sum spectral efficiency of the system with N sub-bands across all users is given by Eq. (21).

$$\Phi_{\text{Sum},N} = \sum_{l=1}^{L} \Phi_{l,N} \tag{21}$$

The advantage of our model in low-SNR regimes stems from its use of the water-filling power allocation strategy, which emphasizes power concentration on high-gain sub-channels rather than uniform spreading. This leads to greater spectral efficiency in noisy environments compared to orthogonal or shared-access systems, where interference or power dilution reduces performance.

2.6 Asymptotic performance

We now analyze the achievable performance of devices operating under wideband conditions $(N \to \infty)$. The instantaneous capacity of user l for a finite number of sub-bands is given Eq. (22), where $p_l(t)$ is subject to the average power constraint presented by Eq. (23).

$$C_{l,\infty} = \int_0^\infty \log_2 \left(1 + \frac{p_l(t) \cdot t}{N_0} \right) f(t)\, dt, \quad \text{for} \quad l = 1, \dots, L \tag{22}$$

$$\int_0^\infty p_l(t) f(t)\, dt = \int_0^\infty \left(\frac{1}{\gamma_0} - \frac{N_0}{t} \right)^+ e^{-t}\, dt = 1 \tag{23}$$

Although this is not a limitation of our approach, from this point onward, we assume that the channel gains are independent and i.i.d. The spectral efficiency of user l under i.i.d. Rayleigh fading is then represented as in Eq. (25), where E_i denotes the exponential integral. The Lagrange multiplier γ_0 satisfies conditions in Eq. (24).

$$C_{l,\infty} = \int_{\gamma_0 N_0}^\infty \log_2 \left(\frac{t}{\gamma_0 N_0} \right) e^{-t}\, dt = \frac{1}{\ln(2)} E_i(\gamma_0 N_0) \tag{24}$$

$$\frac{1}{\gamma_0} \int_0^{+\infty} e^{-t}\, dt - N_0 E_i(\gamma_0 N_0) = 1 \tag{25}$$

Our numerical results show that γ_0 increases as N_0 decreases and γ_0 always lies within the interval [0,1]. In the very high SNR regime, $\gamma_0 \to 1$. In order to characterize the achievable performance in terms of spectral efficiency, we define the capacity across the frequency band W by Eq. (26). Identifying expression Eq. (27) with Eq. (21), we characterize the frequency variation f in terms of the channel gain t as in Eq. (27).

$$C_{l,\infty}(W) = \frac{1}{W} \int_{-\frac{W}{2}}^{\frac{W}{2}} \log_2 \left(1 + \frac{p_l(f) |H_l(f)|^2}{N_0} \right) df \tag{26}$$

$$f = -W e^{-t} + \frac{W}{2} \tag{27}$$

Similarly to the previous section, we define the bandwidth gain factor $\Delta_{l,N}$ as the fraction of the inactive band detected by user l over the total bandwidth W for an infinite number of sub-bands as described by Eq. (28), where Δf represents the frequency interval over which the fading gain is below a

threshold $\gamma_0 N_0$, and asymptotically is presented in Eq. (29).

$$\Delta_{l,N} = \frac{\Delta f}{W} \tag{28}$$

$$\Delta_\infty = 1 - \exp(-\gamma_0 N_0) \tag{29}$$

Consequently, the asymptotic spectral efficiency of user l is represented as in Eq. (30), similar to the fixed number of sub-bands case, when $l = 1$, the spectral efficiency of the horizontal model equals the first user's capacity $C_{1,\infty}$.

$$\Phi_{l,\infty} = \begin{cases} C_{1,\infty}, & \text{if} \quad l = 1 \\ \Delta_\infty \cdot C_{l-1,\infty}, & \text{for} \quad l \in [2, L] \end{cases} \tag{30}$$

It is particularly interesting to quantify the gain in spectral efficiency to show the advantage of using the horizontal model over orthogonal systems. Following the same approach by iterating from user 2 to L, we derive the expression for the total asymptotic spectral efficiency as in Eq. (31).

$$\Phi_{\text{Somme},\infty} = \sum_{l=1}^{L} \Phi_{l,\infty} = \sum_{k=0}^{L-1} \Delta_\infty^k \, C_{1,\infty} = \frac{1-\Delta_\infty^L}{1-\Delta_\infty} C_{1,\infty} \tag{31}$$

Thus, the spectral efficiency sum achieved under the cognitive communication model is greater than or equal to that of the orthogonal model $C_{1,\infty}$. This result highlights the increasing interest in using horizontal models in future wireless communication systems, as the total spectral efficiency always outperforms traditional orthogonal systems. Furthermore, by substituting $C_{1,\infty}$ with its expression from Eq. (25), we obtain the final expression for the achievable spectral efficiency sum (i.e., Eq. (32)), which provides insights into the practical gains achievable by leveraging CR technologies without explicitly knowing the channel gain statistics through γ_0 and the SNR.

$$\Phi_{\text{Somme},\infty} = \frac{1}{\ln(2)} \frac{1-\Delta_\infty^L}{1-\Delta_\infty} E_i(\gamma_0 N_0) \tag{32}$$

3. RESULTS AND DISCUSSION

In this section, we present and analyze the performance evaluation of the proposed horizontal spectrum-sharing model through numerical simulations and theoretical analysis. We compare the spectral efficiency and capacity results of our approach against the conventional orthogonal access method under varying system conditions and SNR levels. The results highlight the advantages of the horizontal model, particularly in low-SNR environments, and confirm the theoretical predictions. Detailed discussions on the impact of the number of secondary users, sub-band allocations, and spectrum utilization efficiency are also provided to offer deeper insights into the system's behavior.

3.1 Performance evaluation

To validate the proposed approach presented in the previous section, we compare the performance of our horizontal spectrum-sharing model against the classical orthogonal access method using numerical results and simulated expressions. The comparison is conducted under varying SNR conditions. For the simulations, we consider $L = 100$ (number of users), $N = 10$ (number of sub-bands), and $M = 10$ (number of secondary users), following the simulation setup commonly used in CR evaluations [20].

The evaluation shows that the horizontal model capacities, minimum (Min_{Horz}), average ($\text{Mean}_{\text{Horz}}$), and maximum ($\text{Max}_{\text{Horz}}$), are consistently greater than those achieved by the orthogonal model (Min_{Orth}, $\text{Mean}_{\text{Orth}}$, Max_{Orth}) in low SNR regions. As SNR increases, the performance of both the horizontal and orthogonal models converges. This will be illustrated in upcoming subsection, which compares their capacities across SNR levels, highlighting the horizontal model's advantage in low-SNR conditions and convergence at high SNR. This comparison justifies that the horizontal model is particularly effective in low SNR or noisy environments, while for higher SNR values, both methods yield similar results. The detailed results are summarized in Table 2, where the minimum, maximum, and average capacities are reported for different SNR levels.

3.2 Example 1: Mathematical explanation

In this subsection, we illustrate the horizontal spectrum-sharing algorithm through a concrete numerical example, as shown in Figure 4 and Figure 5. The top of Figure 4 shows the primary user's occupied sub-bands, which are unavailable for secondary access. Below, the algorithm's behavior is depicted over three consecutive time instants, t, $t + 1$, and $t + 2$, each involving five candidate secondary users. For each time step, the spectral efficiency (denoted by capacity C) of each user is computed based on available sub-bands.

Figure 4 visualizes the dynamic sub-band allocation process across three-time steps, highlighting how secondary users compete for available spectrum. Figure 5 provides a detailed view of the allocation decisions at each step, illustrating the algorithm's efficiency in maximizing spectral utilization without interference. As in Figure 5, the algorithm selects the set of users that maximizes total efficiency while ensuring no sub-band is reused among selected users. The bottom part of the figure shows the final allocation, where four users are chosen to collectively achieve a total spectral efficiency of 11.164.

The algorithm operates sequentially at each time step. First, the primary user selects the sub-band with the highest achievable capacity. Then, each secondary user independently evaluates the spectral efficiency across the remaining available sub-bands and selects the one offering the maximum gain, provided it is not already assigned. This process continues until all users are allocated or no sub-bands remain. The allocation ensures no sub-band reuse, preserving orthogonality across users in each time slot. The overall computational complexity is $O(M \cdot N)$, where M is the number of users and N is the number of sub-bands, since each user performs a linear scan of available sub-bands.

We begin by evaluating the performance of the primary user, who has exclusive access to the channel in the first allocation step. The spectral efficiency achieved is illustrated in Eq. (33). For the first secondary user, five spectral efficiencies corresponding to five candidate sub-bands are computed according to Eq. (34). Among the five sub-bands, sub-band 4 yields the highest capacity and is selected by the first user. Similarly, the second secondary user evaluates the spectral efficiency on each sub-band as in Eq. (35). Here, sub-band 4 is again the optimal choice, although assignment may depend on whether it is already occupied. The third secondary user follows the same procedure as showcased in Eq. (36).

Table 2. Comparison between the capacity values of the two systems

SNR (dB)	Min_{Orth}	$\text{Min}_{\text{Hiers}}$	Max_{Orth}	$\text{Max}_{\text{Hiers}}$	$\text{Mean}_{\text{Orth}}$	$\text{Mean}_{\text{Hiers}}$
0	10.4354	10.6850	11.1851	11.2640	10.7546	10.9123
5	18.6511	18.7831	19.0700	19.0951	18.8301	18.9714
10	29.5776	29.8603	30.1648	30.1834	29.8771	30.0490
15	39.2132	39.6664	39.9552	39.9769	39.6426	39.8404
20	63.3598	63.3598	63.3598	63.3598	63.3598	63.3598

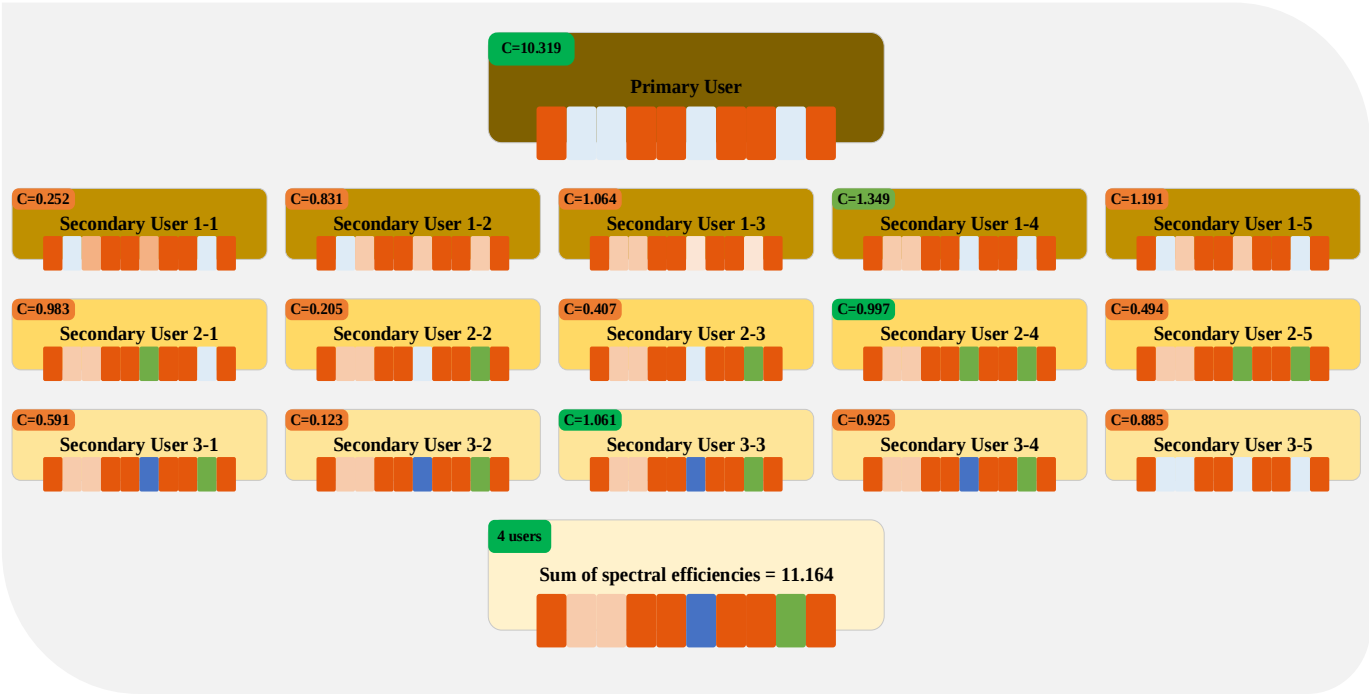

Figure 4. Spectrum-sharing example over three-time steps $(t, t+1, t+2)$ with five candidate secondary users per step and final allocation yields total efficiency of 11.164 with no sub-band reuse

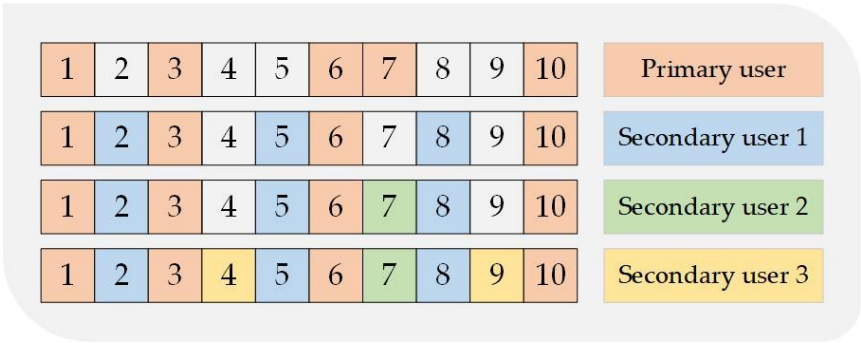

Figure 5. Detailed breakdown of channel allocation and spectrum filling process

$$C_{\max}^{\text{PU}} = 10.319 \tag{33}$$

$$\begin{cases} C_{1,1} = 0.252 \\ C_{1,2} = 0.831 \\ C_{1,3} = 1.064 \\ C_{1,4} = 1.349 \\ C_{1,5} = 1.191 \end{cases} \Rightarrow C_{\max}^{(1)} = \max\left(C_{1,i}\right) = C_{1,4} = 1.349 \tag{34}$$

$$\begin{cases} C_{2,1} = 0.983 \\ C_{2,2} = 0.205 \\ C_{2,3} = 0.407 \\ C_{2,4} = 0.997 \\ C_{2,5} = 0.494 \end{cases} \Rightarrow C_{\max}^{(2)} = \max\left(C_{2,i}\right) = C_{2,4} = 0.997 \tag{35}$$

$$\begin{cases} C_{3,1} = 0.591 \\ C_{3,2} = 0.123 \\ C_{3,3} = 1.061 \\ C_{3,4} = 0.925 \\ C_{3,5} = 0.885 \end{cases} \Rightarrow C_{\max}^{(3)} = \max\left(C_{3,i}\right) = C_{3,3} = 1.061 \tag{36}$$

Sub-band 3 is identified as the most favorable for user 3. Thus, it is chosen if not already claimed by a previous user. The system in this example includes a total of $L = 4$ users: one primary and three secondaries. The aggregate system performance is measured by summing the maximum capacities of all users as presented by Eq. (37). This total capacity reflects the effectiveness of the horizontal model in maximizing spectral efficiency without overlap in

transmission.

$$\Phi_{\text{sum}} = C_{\max}^{\text{PU}} + C_{\max}^{(1)} + C_{\max}^{(2)} + C_{\max}^{(3)} = 11.164 \quad (37)$$

To formalize the sub-band allocation process described above, we present a simplified pseudocode representation of the horizontal spectrum-sharing strategy in Algorithm 1. This algorithm outlines how each user sequentially selects the most efficient available sub-band, ensuring non-overlapping assignments and maximizing total spectral efficiency.

3.3 Example 2: Mathematical explanation

In this subsection, we present a detailed explanation of the horizontal spectrum-sharing algorithm through a second numerical example that spans two sequential time steps, t and $t+1$. The process is illustrated in Figures 6 and 7, which depict how sub-bands are dynamically and efficiently assigned to secondary users over time. Each user selects the sub-band offering the highest spectral efficiency while ensuring that no sub-band is reused, thereby avoiding interference. Figure 7 provides a step-by-step view of sub-band allocation across two-time steps, illustrating how the algorithm avoids overlap and maximizes spectral efficiency through sequential user selection.

This example highlights the temporal coordination of users and the algorithm's ability to sustain high cumulative efficiency in multi-user environments. We begin by evaluating the performance of the primary user, who again initiates the spectrum allocation by fully utilizing one available sub-band. The spectral efficiency achieved in this instance is shown in Eq. (38).

$$C_{\max}^{\text{PU}} = 10.609 \quad (38)$$

Next, we compute the individual spectral efficiencies for the first secondary user over five candidate sub-bands. As indicated in Eq. (39), sub-band 1 yields the highest value and is selected.

$$\begin{cases} C_{1,1} = 1.321 \\ C_{1,2} = 0.925 \\ C_{1,3} = 0.928 \\ C_{1,4} = 1.167 \\ C_{1,5} = 0.896 \end{cases} \Rightarrow C_{\max}^{(1)} = \max\left(C_{1,i}\right) = C_{1,1} = 1.321 \quad (39)$$

The second secondary user performs a similar evaluation. Based on Eq. (40), the highest spectral efficiency is achieved on sub-band 4.

$$\begin{cases} C_{2,1} = 0.485 \\ C_{2,2} = 0.301 \\ C_{2,3} = 0.370 \\ C_{2,4} = 2.204 \\ C_{2,5} = 1.493 \end{cases} \Rightarrow C_{\max}^{(2)} = \max\left(C_{2,i}\right) = C_{2,4} = 2.204 \quad (40)$$

In total, this example includes $L = 3$ users: one primary and two secondaries. The overall performance of the system is captured by summing the maximum achievable spectral efficiencies, as shown in Eq. (41).

$$\Phi_{\text{sum}} = C_{\max}^{\text{PU}} + C_{\max}^{(1)} + C_{\max}^{(2)} = 11.358 \quad (41)$$

This confirms the capacity gain resulting from the use of a horizontal spectrum-sharing strategy, enabling each user to access unoccupied sub-bands with optimized efficiency while avoiding collisions.

Algorithm 1. Sub-band allocation with horizontal spectrum sharing over three-time steps

Input: Spectral efficiencies $C_{\{i,u\}}^{t}$ for user u on sub-band i at each time step $t \in \{1,2,3\}$
Initialize: Total spectral efficiency $\Phi_{sum} \leftarrow 0$
for each time step t = 1 to 3 do
  Assigned sub-bands at time t: $B^t \leftarrow \emptyset$
  Primary user selects $i* = argmax_{\{i \notin B^t\}}\left(C_{\{i,PU\}}^{t}\right)$
  Assign sub-band $i*$ to primary user
  Update $\Phi_{sum} \leftarrow \Phi_{sum} + C_{\{i*,PU\}}^{t}$
  Update $B^t \leftarrow B^t \cup \{i*\}$
  for each secondary user $u = 1$ to number of secondary users do
    Evaluate $C_{\{i,u\}}^{t}$ for all available sub-bands $i \notin B^t$
    Select $i* = argmax_{\{i \notin B^t\}}\left(C_{\{i,u\}}^{t}\right)$
    if such i* exists then
      Assign sub-band i* to user u
      $Update\ \Phi_{sum} \leftarrow \Phi_{sum} + C_{\{i*,u\}}^{t}$
      $Update\ B^t \leftarrow B^t \cup \{i*\}$
    end if
  end for
end for
Output: Φ_{sum}

Algorithm 2. Sub-band allocation over two-time steps with horizontal spectrum sharing

Input: Spectral efficiencies $C_{\{i,u\}}^{t}$ for user u on sub-band i at time t
Initialize: Assigned sub-bands $B^t \leftarrow \emptyset$, Total capacity $\Phi_{sum} \leftarrow 0$
for each time step t = 1 to 2 do
  Primary user selects sub-band $i* = argmax_{\{i \notin B^t\}} C_{\{i,PU\}}^{t}$
  Assign sub-band $i*$ to primary user
  Update $\Phi_{sum} \leftarrow \Phi_{sum} + C_{\{i*,PU\}}^{t}$
  Update $B^t \leftarrow B^t \cup \{i*\}$
  for each secondary user u = 1 to number of secondary users do
    Evaluate $C_{\{i,u\}}^{t}$ for all $i \notin B^t$
    Select sub-band $i* = argmax_{\{i \notin B^t\}} C_{\{i,u\}}^{t}$
    if such $i*$ exists then
      Assign sub-band $i*$ to user u
      Update $\Phi_{sum} \leftarrow \Phi_{sum} + C_{\{i*,u\}}^{t}$
      Update $B^t \leftarrow B^t \cup \{i*\}$
    end if
  end for
end for
Output: Φ_{sum}

We now illustrate a two-time-step spectrum-sharing scenario that includes a primary user and two secondary users. As before, the primary user initiates the process by occupying one of the available sub-bands to maximize its own spectral efficiency. The subsequent allocation at each time step is performed by the secondary users, who select the sub-band

offering the highest spectral efficiency from a fixed set of five candidates. Each allocation strictly avoids sub-band reuse to prevent interference. The efficiency obtained by the primary user is shown in Eq. (6), followed by the computed efficiencies for each secondary user in Eqs. (7) and (8), respectively. The total achieved efficiency for this two-step allocation process is summarized in Eq. (9), highlighting the gain in capacity and spectrum utilization.

3.4 Performance analysis under different SNR conditions

Before delving into the detailed analysis of varying SNR levels and user density, Figure 8 offers a foundational comparison between orthogonal and horizontal spectrum access strategies in terms of spectral efficiency. Specifically, Figure 8(a) illustrates the performance of the orthogonal access model, where each user is allocated a dedicated sub-band, ensuring interference-free transmission but resulting in inefficient spectrum utilization under light user loads. In contrast, Figure 8(b) presents the horizontal access approach, which allows users to dynamically and opportunistically share spectrum, leading to higher spectral efficiency across the user index range.

To facilitate direct comparison, Figure 8(c) overlays the spectral efficiency profiles of both models. The results clearly show that the horizontal model consistently outperforms the orthogonal one, especially in scenarios with partial spectrum occupancy, where the flexibility of dynamic access enables better exploitation of spectral opportunities. This initial observation establishes a baseline understanding of the relative benefits of each model and sets the stage for more comprehensive analyses in the subsequent sections, where the effects of SNR variations and increasing user density are systematically explored.

Figure 9(a) presents the comparison of the total spectral efficiency for two different configurations: an orthogonal system and a horizontal system, considering $L = 10$ and $L = 50$ with a fixed number of sub-bands $N = 16$. It is evident that the spectral efficiency of the horizontal system is significantly higher compared to the orthogonal system. The maximum spectral efficiency of the orthogonal system cannot exceed approximately 60% when the configuration includes 10 users. At higher SNR values, the spectral efficiencies of both systems tend to converge. However, at very high SNR, the total capacity sum approaches $C_{1,\infty}$. This result is intuitive, since in the high SNR regime, the water-filling level $1/\gamma_0$ becomes larger than the channel noise term σ^2/h^2, leading to the pouring of more power as SNR increases, and thus the sum spectral efficiency $\Phi_{\text{Somme},\infty} \to 1$. In Figure 9(b), we observe the difference in spectral efficiency between the horizontal systems with $M = 10$ and $M = 50$ and the orthogonal system. As shown, the spectral efficiency for 50 users is greater than that for 10 users, highlighting the effect of increased competition among cognitive users. This result emphasizes that a higher number of cognitive users improves the overall spectral efficiency of the system.

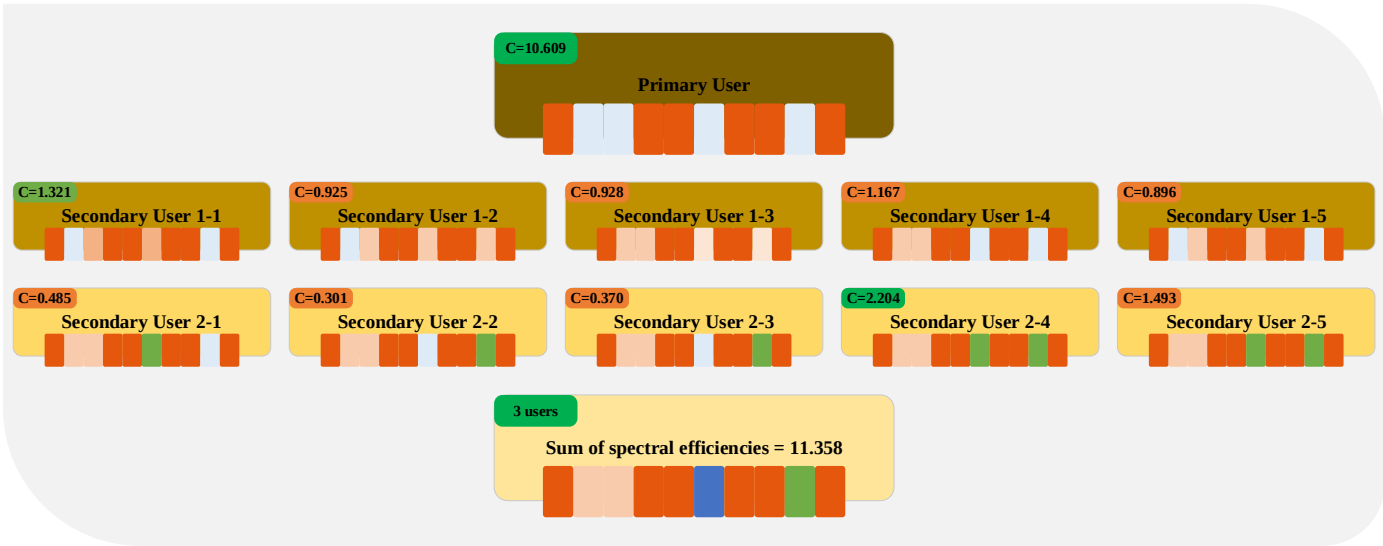

Figure 6. Spectrum-sharing example over two-time steps (t and $t + 1$) with five candidate secondary users per step, and final allocation yields a cumulative spectral efficiency of 11.358 with no sub-band reuse

Figure 7. Detailed breakdown of sub-band allocation and channel filling process across time steps t and $t + 1$, illustrating interference-free sharing

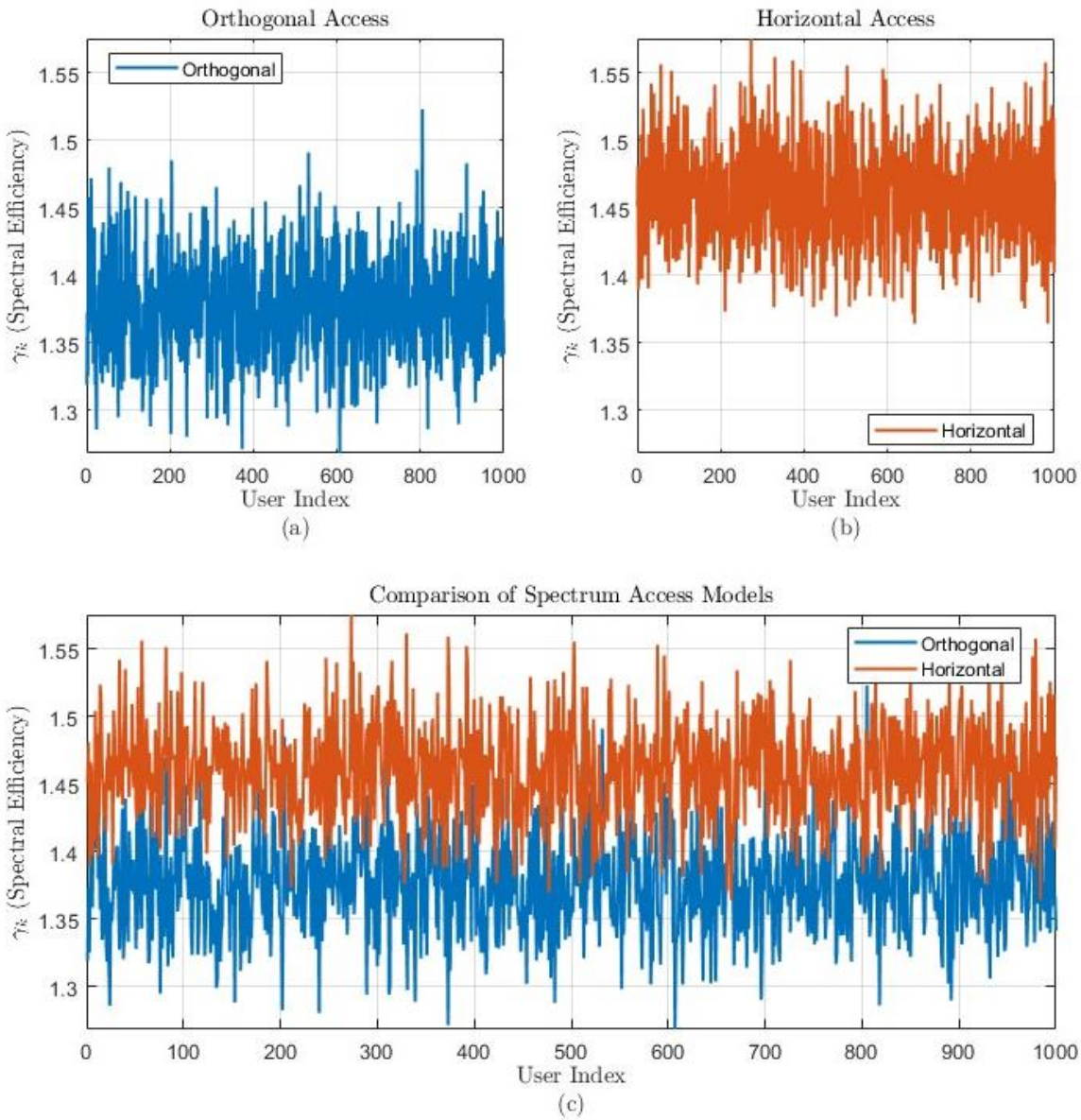

Figure 8. Comparison between the capacities of the orthogonal and horizontal models: (a) Capacity of orthogonal model; (b) Capacity of Horizontal model; (c) Comparisons between orthogonal and Horizontal models

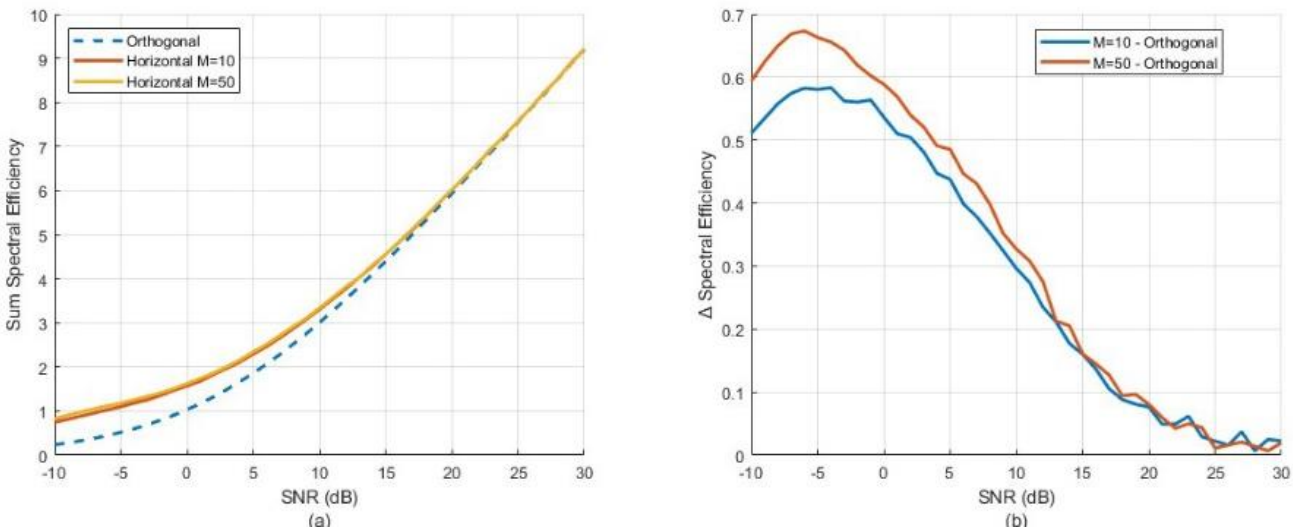

Figure 9. Comparison between the spectral efficiency sum of an orthogonal system and horizontal systems with varying numbers of candidate secondary users

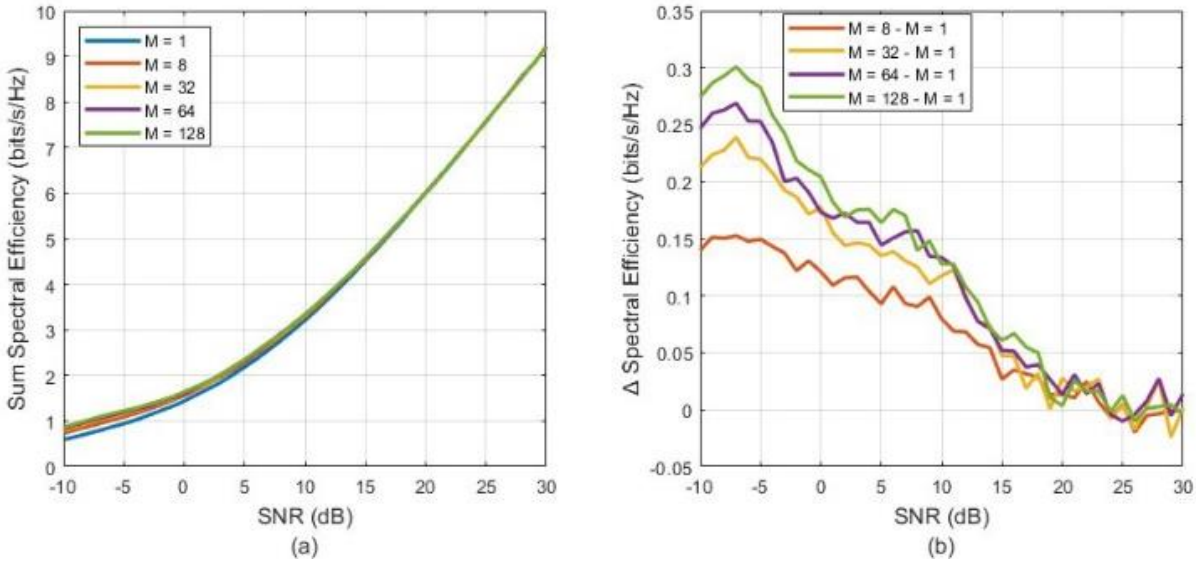

Figure 10. The spectral efficiency sums of a system with $N = 16$ sub-bands

To further illustrate the benefits of our algorithm in terms of spectral efficiency, a comparison is performed between the orthogonal spectrum access strategy (where only one secondary user accesses the spectrum at a time, $M = 1$) and the horizontal spectrum access scheme (where multiple secondary users contend in parallel) for various values of M, as a function of the SNR in decibels. To ensure statistical reliability in the presence of random channel power gains, the reported results represent the average over 1000 successive spectrum access events (Figure 10). We use 1000 Monte Carlo iterations to ensure statistically stable average performance, in line with standard practice in CR evaluations [20].

As depicted in Figure 10(a), the horizontal access mechanism significantly improves the total system spectral efficiency compared to the orthogonal access method. Increasing the number of candidate secondary users M generally leads to better performance, as it raises the probability of finding a user with a favorable channel condition, thereby enabling more efficient spectrum usage.

However, as shown in Figure 10(b), the performance gain relative to the baseline case $M = 1$ grows at a diminishing rate. The initial increase (e.g., from $M = 1$ to $M = 8$) yields a substantial boost in spectral efficiency, while further increases (e.g., to $M = 64$ or $M = 128$) provide progressively smaller improvements. This diminishing return effect becomes even more pronounced at higher SNR levels. In high-SNR regimes, the primary user tends to occupy more sub-bands, leaving less spectrum for secondary users to access. As a result, the performance gap between horizontal and orthogonal access narrows in such scenarios. The convergence of performance between the horizontal and orthogonal models at high SNR is consistent with the behavior of the water-filling strategy, which tends to allocate power more uniformly across sub-bands as the signal dominates noise. In such conditions, the benefit of exclusive sub-band access diminishes, and both models approach the theoretical capacity limit of the channel [16, 17].

4. CONCLUSIONS

In this work, we analyzed a CR system in which cognitive users opportunistically access available spectrum to improve overall spectral utilization. We introduced a horizontal spectrum-sharing model that enables decentralized sub-band allocation based on real-time channel conditions, offering an alternative to traditional orthogonal access. The model promotes exclusive sub-band use without centralized scheduling, enhancing spectral efficiency, particularly in low-SNR regimes, while maintaining scalability as the number of users increases. Simulations confirmed that the horizontal model consistently outperforms orthogonal allocation, with both models converging at high SNR where interference becomes negligible. These results are promising for dense and dynamic wireless environments. From a practical standpoint, applying this model in real-world systems requires consideration of existing regulatory frameworks and standardization constraints. While the model is well suited for decentralized operation, regulatory policies must accommodate flexible and dynamic spectrum access while ensuring interference protection and coexistence with licensed systems. Current wireless standards such as those used in 5G networks emphasize controlled and managed spectrum usage, and adopting opportunistic models may require protocol adaptations to support real-time coordination. This study also makes some simplifying assumptions, including perfect spectrum sensing, static primary users, and centralized user selection, which may limit immediate practical deployment. In reality, factors such as mobility, sensing inaccuracies, and the need for distributed decision-making play critical roles. Future work will address these limitations by incorporating more realistic conditions and exploring adaptive, learning-based methods for decentralized coordination. Overall, the proposed horizontal model offers a flexible and efficient approach for advancing spectrum sharing in next-generation CR systems.

REFERENCES

[1] Farhi, H., Messai, A. (2020). Spectral capacity in cognitive networks. In Proceedings of the 8th International Conference on Sciences of Electronics, Technologies of Information and Telecommunications (SETIT'18). https://doi.org/10.1007/978-3-030-21009-

0_41
[2] Muzaffar, M.U., Sharqi, R. (2024). A review of spectrum sensing in modern cognitive radio networks. Telecommunication Systems, 85: 347-363. https://doi.org/10.1007/s11235-023-01079-1
[3] Askari, M., Dastanian, R. (2023). An optimized spectrum sharing scheme for cognitive radio. Wireless Networks, 29: 1621-1627. https://doi.org/10.1007/s11276-022-03193-5
[4] Bai, W., Zheng, G., Xia, W., Mu, Y., Xue, Y. (2025). Multi-user opportunistic spectrum access for cognitive radio networks based on multi-head self-attention and multi-agent deep reinforcement learning. Sensors, 25(7): 2025. https://doi.org/10.3390/s25072025
[5] Abdulkadir, Y., Simpson, O., Sun, Y. (2024). Opportunistic interference alignment in cognitive radio networks with space–time coding. Journal of Sensor and Actuator Networks, 13(5): 46. https://doi.org/10.3390/jsan13050046
[6] Bouhafs, F., Raschellà, A., Mackay, M., den Hartog, F. (2022). A spectrum management platform architecture to enable a sharing economy in 6G. Future Internet, 14(11): 309. https://doi.org/10.3390/fi14110309
[7] Nasser, A., Al Haj Hassan, H., Abou Chaaya, J., Mansour, A., Yao, K.C. (2021). Spectrum sensing for cognitive radio: Recent advances and future challenge. Sensors, 21(7): 2408. https://doi.org/10.3390/s21072408
[8] Meng, Y., Qi, P., Lei, Q., Zhang, Z., Ren, J., Zhou, X. (2022). Electromagnetic spectrum allocation method for multi-service irregular frequency-using devices in the space–air–ground integrated network. Sensors, 22(23): 9227. https://doi.org/10.3390/s22239227
[9] Fraz, M., Muslam, M.M.A., Hussain, M., Amin, R., Xie, J. (2023). Smart sensing enabled dynamic spectrum management for cognitive radio networks. Frontiers in Computer Science, 5: 1271899. https://doi.org/10.3389/fcomp.2023.1271899
[10] Wu, J., Qiu, Z., Dai, M., Bao, J., Xu, X., Cao, W. (2024). Distributed sequential detection for cooperative spectrum sensing in cognitive Internet of Things. Sensors, 24(2): 688. https://doi.org/10.3390/s24020688
[11] Du, H., Wang, Y. (2024). A double-threshold cooperative spectrum sensing algorithm in the Internet of Vehicles. World Electric Vehicle Journal, 15(5): 195. https://doi.org/10.3390/wevj15050195
[12] Patil, A., Iyer, S., López, O.L.A., Pandya, R.J., Pai, K., Kalla, A., Kallimani, R. (2024). A comprehensive survey on spectrum sharing techniques for 5G/B5G intelligent wireless networks: Opportunities, challenges and future research directions. Computer Networks, 253: 110697. https://doi.org/10.1016/j.comnet.2024.110697
[13] Talekar, S. (2022). Applications of cognitive radio networks: A review. Journal of ISMAC, 4(4): 272-283. https://doi.org/10.36548/jismac.2022.4.004
[14] Akyildiz, I.F., Lo, B.F., Balakrishnan, R. (2011). Cooperative spectrum sensing in cognitive radio networks: A survey. Physical Communication, 4(1): 40-62. https://doi.org/10.1016/j.phycom.2010.12.003
[15] Yazdani, H., Vosoughi, A., Gong, X. (2021). Achievable rates of opportunistic cognitive radio systems using reconfigurable antennas with imperfect sensing and channel estimation. IEEE Transactions on Cognitive Communications and Networking, 7(3): 802-817. https://doi.org/10.1109/TCCN.2021.3056691
[16] Zhang, J., Wen, C.K., Jin, S., Gao, X., Wong, K.K. (2013). On capacity of large-scale MIMO multiple access channels with distributed sets of correlated antennas. IEEE Journal on Selected Areas in Communications, 31(2): 133-148. https://doi.org/10.1109/JSAC.2013.130203
[17] Chen, X., Jing, T., Huo, Y., Li, W., Cheng, X., Chen, T. (2012). Achievable transmission capacity of cognitive radio networks with cooperative relaying. In Proceedings of the 7th International ICST Conference on Cognitive Radio Oriented Wireless Networks and Communications (CROWNCOM), Stockholm, Sweden, pp. 1-6.
[18] Balachander, T., Krishnan, M.B.M. (2022). Efficient utilization of cooperative spectrum sensing (CSS) in cognitive radio network (CRN) using non-orthogonal multiple access (NOMA). Wireless Personal Communications, 127: 2189-2210. https://doi.org/10.1007/s11277-021-08776-7
[19] Meng, F., Wang, Y., Zhang, L., Zhao, Y. (2023). Joint detection algorithm for multiple cognitive users in spectrum sensing. arXiv preprint, arXiv:2311.18599. https://doi.org/10.48550/arXiv.2311.18599
[20] El-haryqy, N., Madini, Z., Zouine, Y. (2024). A review of deep learning techniques for enhancing spectrum sensing and prediction in cognitive radio systems: Approaches, datasets, and challenges. International Journal of Computers and Applications, 46(12): 1104-1128. https://doi.org/10.1080/1206212X.2024.2414042

NOMENCLATURE

$C_{l,\infty}$	Average capacity of user l (bits/s/Hz) under continuous fading
$C_{l,N}$	Instantaneous capacity of user l over N sub-bands
$\Phi_{l,N}$	Spectral efficiency per band for user l over N sub-bands
$\Phi_{\mathrm{Sum},N}$	Total spectral efficiency over all users and sub-bands
$\Delta_{l,N}$	Bandwidth gain factor for user l
$p_l(t)$	Power allocated by user l as a function of fading t
p_l^i	Power allocated by user l on sub-band i
p_{l-1}^i	Power allocated by user $l-1$ on sub-band i
N_0	Noise power spectral density (W/Hz)
h_l^i	Channel gain for user l on sub-band i
y_{RI}^i	Received signal at receiver on sub-band i
$y_l^i(k)$	Received signal at user l, sub-band i, time k
$c_{l-1,l}^i(k)$	Channel coefficient from user $l-1$ to l, sub-band i
s_l^i, $s_{l-1}^i(k)$	Transmitted signal from user l or $l-1$
n_l^i, $n_{l-1}^i(k)$	Additive WHITE GAUSSIAN NOISE (AWGN)
γ_0	Water-filling cut-off level
$\bar{P}$	Power budget (normalized to 1)
Ψ_l	Set of sub-bands sensed as occupied by user l
Ω_l	Set of available sub-bands for user l
N	Total number of sub-bands
L	Total number of users
T	Transmission period
βT	Coherence time of the fading channel

M	Number of detection time samples ($M = \beta T$)
$\mathrm{card}(\cdot)$	Cardinality of a set
$E_i(\cdot)$	Exponential integral function
f	Frequency variable

Greek symbols

l	Index for user l
i	Index for sub-band i
RI	Refers to the receiver
k	Discrete time index
nf	Nanofluid or normalized-fading (context-dependent)